# INFLUENCE OF ARMOURED VEHICLE'S BOTTOM SHAPE ON THE PRESSURE IMPULSE

**Wiesław Barnat, Robert Panowicz**
**Tadeusz Niezgoda**

*Military University of Technology, Faculty of Mechanical Engineering*
*Department of Mechanics and Applied Computer Science*
*Gen. S. Kaliskiego Street 2, 00-908 Warsaw, Poland*
*tel.: +48 22 6839849, fax: +48 22 6839355*
*e-mail: wbarnat@wat.edu.pl, e-mail: tniezgoda@wat.edu.pl*

***Abstract***

*This paper presents the results of a numerical analysis of military vehicles hulls mine resistance. The research concerns armours loaded with blast wave from large IED charges in three cases. First is an explosion in Euler domain without any boundary conditions. Second consists of Euler domain with flat bottom and the ground. Third is simulated Euler domain with ground and deflector. Boundary conditions used both in second and third case resulted in growth of the pressure impulse due to the reflection from a rigid obstacle. In the article different hull bottom shapes are compared. The gap between the bottom and the ground is fixed in all cases. Explosion in Euler domain without limitations is added as a reference.*

*The blast wave caused by the detonation (simulated as a point detonation) propagated in cubic mesh with appropriate boundary conditions. Theoretical solution of spherical non-linearity is given in a form of Taylor equations. It was used to verify the numerical model.*

*The research showed that the ground proximity affects the results of the simulation. The pressure impulse is amplified due to the wave reflection from both the bottom of the vehicle and the ground. As well as that, the study confirmed that the usage of the deflector considerably reduces the impact load to the structure.*

***Keywords:*** *IED, improvised explosive device, mine resistance, armour, deflector, hull design, light armoured vehicle*

## 1. Introduction

Light armoured vehicles are threatened by most weapons available for the opposing forces among which are anti-tank mines and Improvised Explosive Devices (IEDs). These threats led to introducing new technical and tactical requirements for hull design allowing high survivability on the battlefield. This goal is achieved by:

- proper hull geometry ensuring sufficient protection level,
- suspension designed to sustain external dynamic loads,
- mine resistance at level that provides crew and equipment safety while attacked with large and differently placed explosives.

Modern technology allows proper shaping and configuration of armoured hulls both with regards to material properties and geometry. Recent development of numerical methods and increase of computers performance allowed modelling many physical phenomena, ranging from combustion of the explosive to simulation of the blast wave effect on a structure. As well as factors mentioned above, nowadays there is more interest in passive protection techniques [2, 3]. Therefore, researchers work intensively on new design solutions not only using empirical techniques, but also numerical experiments. The aim is to obtain maximum possible anti-mine protection level for the crew and equipment [1] against mines and IEDs.

In presented study a coupling algorithm to combine Euler and Lagrange domain was used. First domain is used to model the blast wave and the air in which the wave propagates, whereas second describes the structure using mass, momentum and energy conservation laws. It must be stated,

that the issue of detonation is a complex problem. Therefore, a special modelling technique was used. The algorithms and techniques used for blast modelling are broadly discussed in the literature [4, 5, 6, 8].

A graphical illustration of primary pressure wave propagation is presented in Fig. 1. It shows subsequent stages of spherical wave.

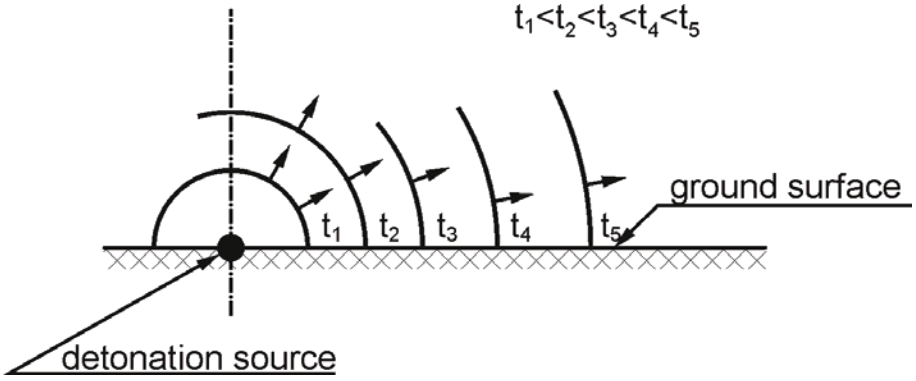


*Fig. 1. Primary pressure wave propagation [8]*

In case of multiple reflections from vehicle's bottom and the ground, pressure wave is amplified. One of possible solutions is to introduce graphical method of apparent source. The technique to construct the wave front using apparent source method is shown in Fig. 2 [8]. The method was also used in previous studies concerning multiple reflections. It was discussed broader in [12].

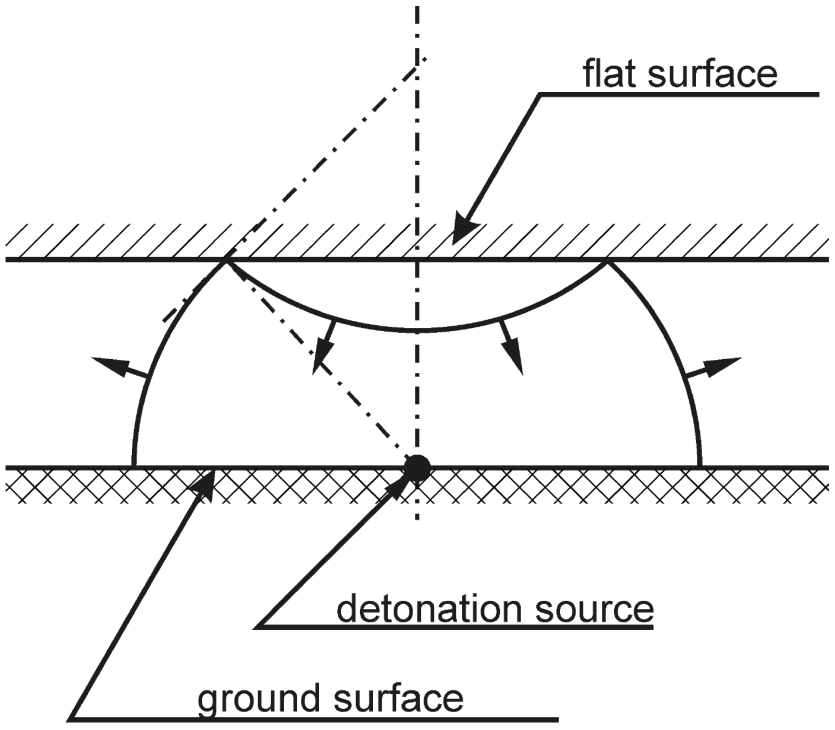


*Fig. 2. Construction of reflected wave's front using apparent source method [8]*

As previously mentioned, simulation of multiple reflection between flat bottom and the ground is complicated. Such a reflection results in the creation of Mach's wave. It arises from intersection of incident and reflected wave (point a in Fig. 3). This wave is flat and perpendicular to reflecting surface. Mach waves are rare phenomena and have been used in strong nuclear explosions to enhance destructive power.

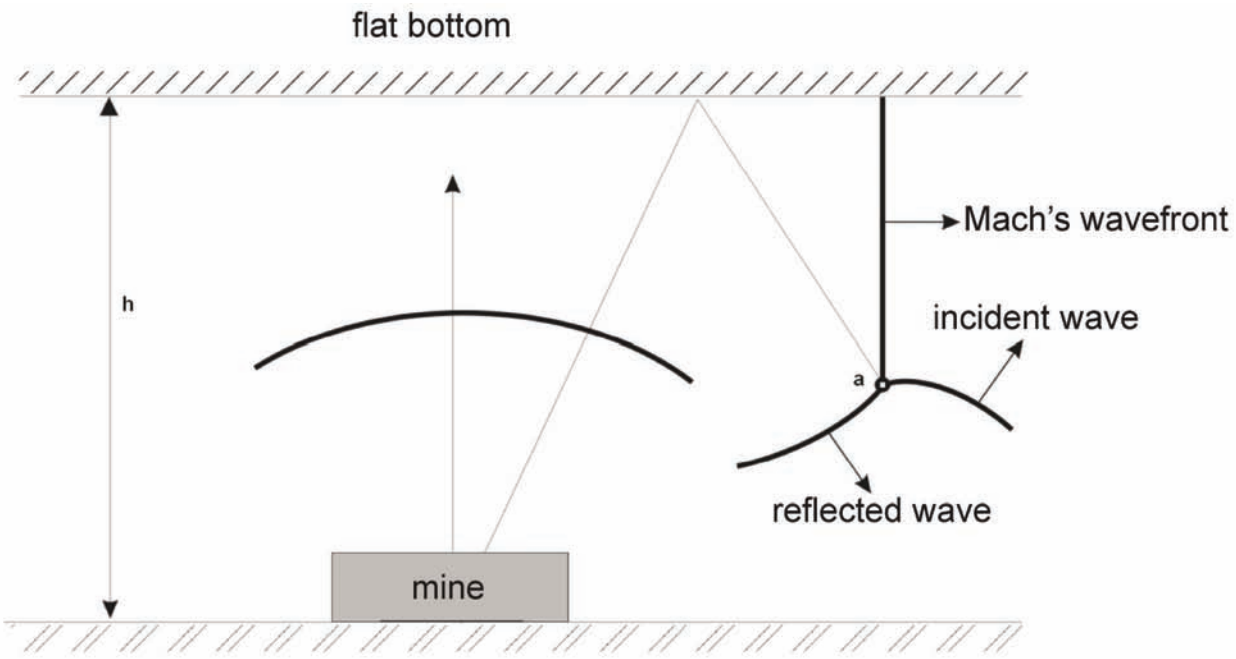


*Fig. 3. Mach wave creation*

In order to simulate the bottom of a vehicle and the ground, appropriate constitutive models were chosen. Those models are implemented in MSC Dytran software [7]. During the calculation a uniform explicit algorithm of integration of movement motions over time was used. The aim of the research was to examine how the bottom's shape affects the pressure distribution and its maximum values.

## 2. Numerical models

All tests concerning military vehicles mine resistance are conducted using NATO STANAG 4569 standardization. One of possible experiments is to examine the effects of TM 57 anti-tank mine detonation. The mine contains 6,34 kg TNT. However, Improvised Explosive Devices often have mass greater than standard mine. Consequently, numerical tests of detonation were also held using bigger charges. The analysis was conducted for three different numerical models:

- model 1 – Euler domain without any boundary conditions,
- model 2 – Euler domain with flat bottom of the vehicle and the ground,
- model 3 – Euler domain with Hull equipped with deflector and the ground.

In the second and third model the gap between the bottom and the ground was identical. First model was used as a reference to compare the pressure impulse of reflected wave in other models.

The blast wave caused by the detonation (simulated as point source detonation) propagated in cubic domain with appropriate boundary conditions. Theoretical solution of non-linear spherical wave front exists as Taylor equation [9, 10]:

$$p(r) = 0{,}155\, E_o\, r^{-3}\,, \tag{1}$$

where:
$E_o$ – initial internal energy,
r – actual sphere radius.

Such an approach allows computer modelling of the blast wave propagation phenomenon by applying initial conditions (density, energy, pressure) to certain Euler cells. Then, such defined

system of mass, momentum and energy equations can be solved. Typical values for explosive substance are density 1600 kg/m3 and initial specific energy 4,2 kJ/kg.

Euler domain consisted of Hex 8 elements with ideal gas properties ($\gamma = 1{,}4$ and density $\rho = 1{,}2829$ kg/m3). General outlook of the investigated system is presented in the Fig. 4.

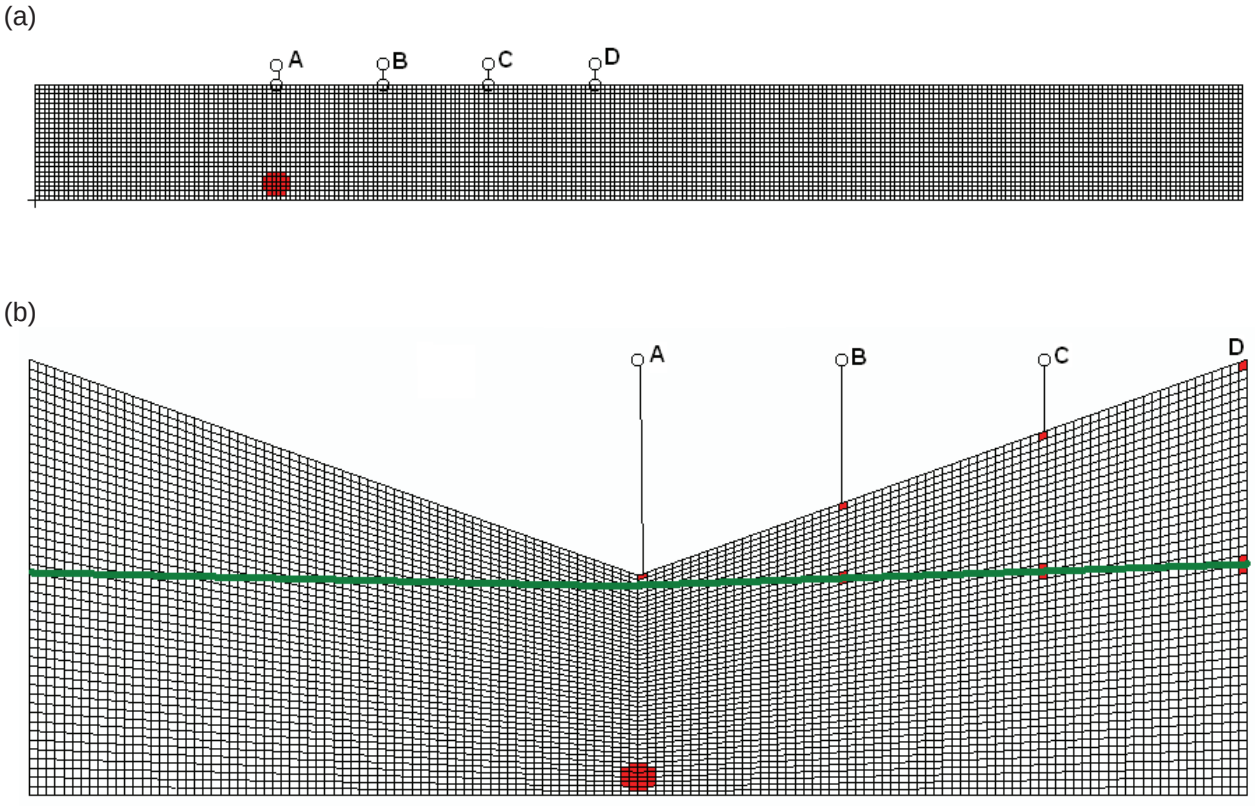


*Fig. 4. Vehicle's bottom: a) flat bottom [12], b) with deflector*

In the Fig. 4, there are presented characteristic Euler cells (A, B, C, D) for both cases. In these cells the values of pressure affecting vehicle's bottom was measured. Due to the thick bottom (preventing the deformation) a maximum pressure impulse gain was assumed to occur. Additionally, a thick green line in Fig. 4 (b) is a flat bottom's outline.

In all considered models structural nodes did not have initial conditions applied. Therefore, all velocities and displacements were equal to zero.

## 3. Results and discussion

As a result of the analyzes, plots of pressure distribution for characteristic points and pressure maps for entire models were obtained.

Pressure plot for Model 1 is depicted in Fig. 5. At The maximum pressure of free wave occurred in cell A and reached the value of 1,15E9 Pa. Then, due to wave propagation, the pressure value decreased to 8,2E8 Pa in cell B. Consequently, for cell C pressure value was 4,4E8 Pa and for cell D 2,3E8 Pa.

Plot of pressure change for chosen Euler cells in Model 2 is show in Fig. 6. At the beginning, the maximum pressure in cell A reached a value 4,7E9 Pa, which was four times larger that in Model 1. It is due to the fact, that the wave was reflected from a rigid obstacle – the ground. Then, the pressure value decreased to 3,5E9 Pa in cell B. It was 4,2 times more than in cell B in Model 1. Pressure in cell C was 1,5E9 Pa which is 3,4 times more than in Model 1.Finally, pressure in cell D is 5,5E8 Pa and was two times bigger than in Model 1.

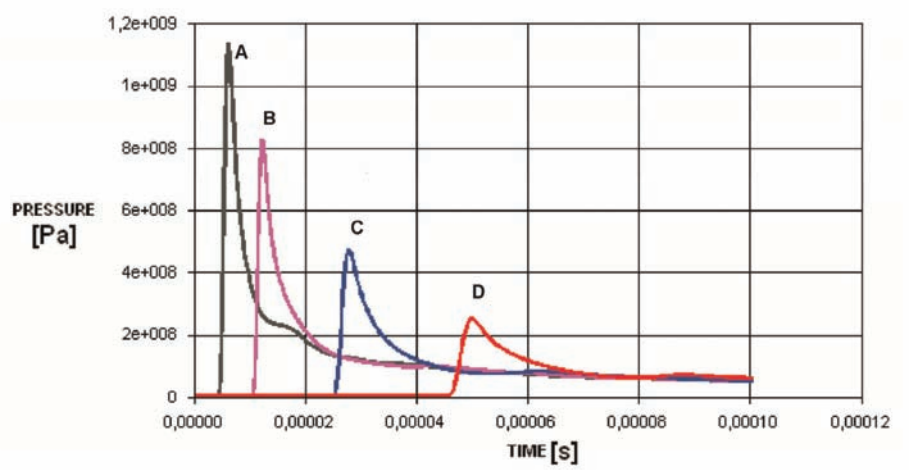


*Fig. 5. Model 1 – pressure values in cells A, B, C and D [12]*

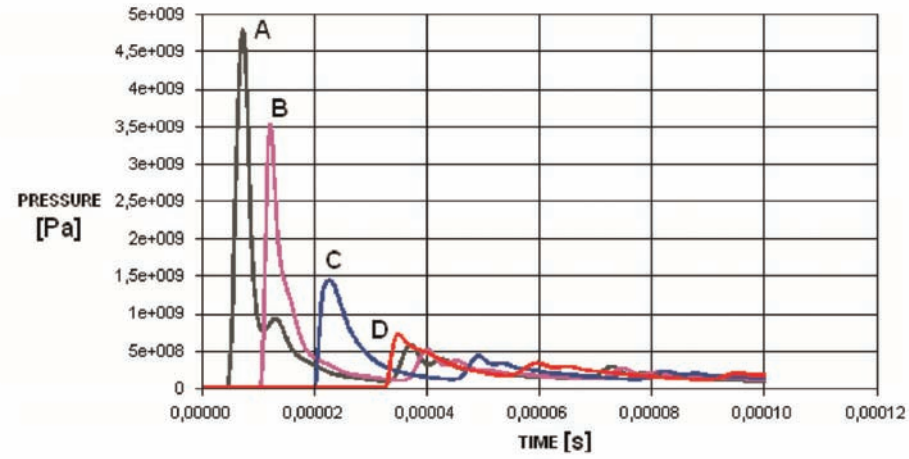


*Fig. 6. Model 2 – pressure values in cells A, B, C and D [12]*

Figure 7 depicts multiple reflections in Model 2. For the time t = 4,44E6 s blast wave reached the ground and reflected. Such a situation occurs when, a mine is detonated in concrete stand. In Fig. 7 (a) the first pressure reflection is shown, resulting in pressure gain to the value of 4,81 E9 Pa. Later, for time t = 8,7 E-6 s pressure wave reached the flat bottom. As a result of reflection from rigid wall (Fig. 7 (c), t = 1E-5 s) the pressure wave was amplified 2,5 times . Later propagation of the blast wave is show on Fig. 7 (d) – (f). Additionally, Fig 7 (h) presents reflection from the ground. Figure 7 (g) and (h) present the creation of Mach's wave as a result of multiple reflections and intersection between incident and reflected waves.

(a) (b)

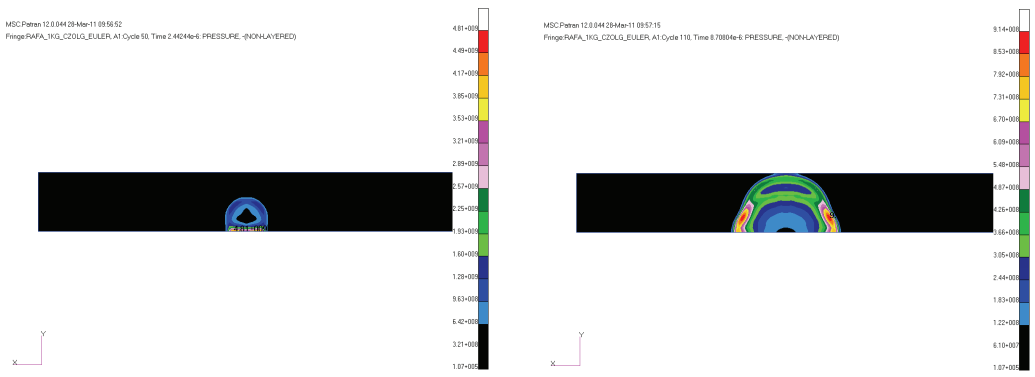

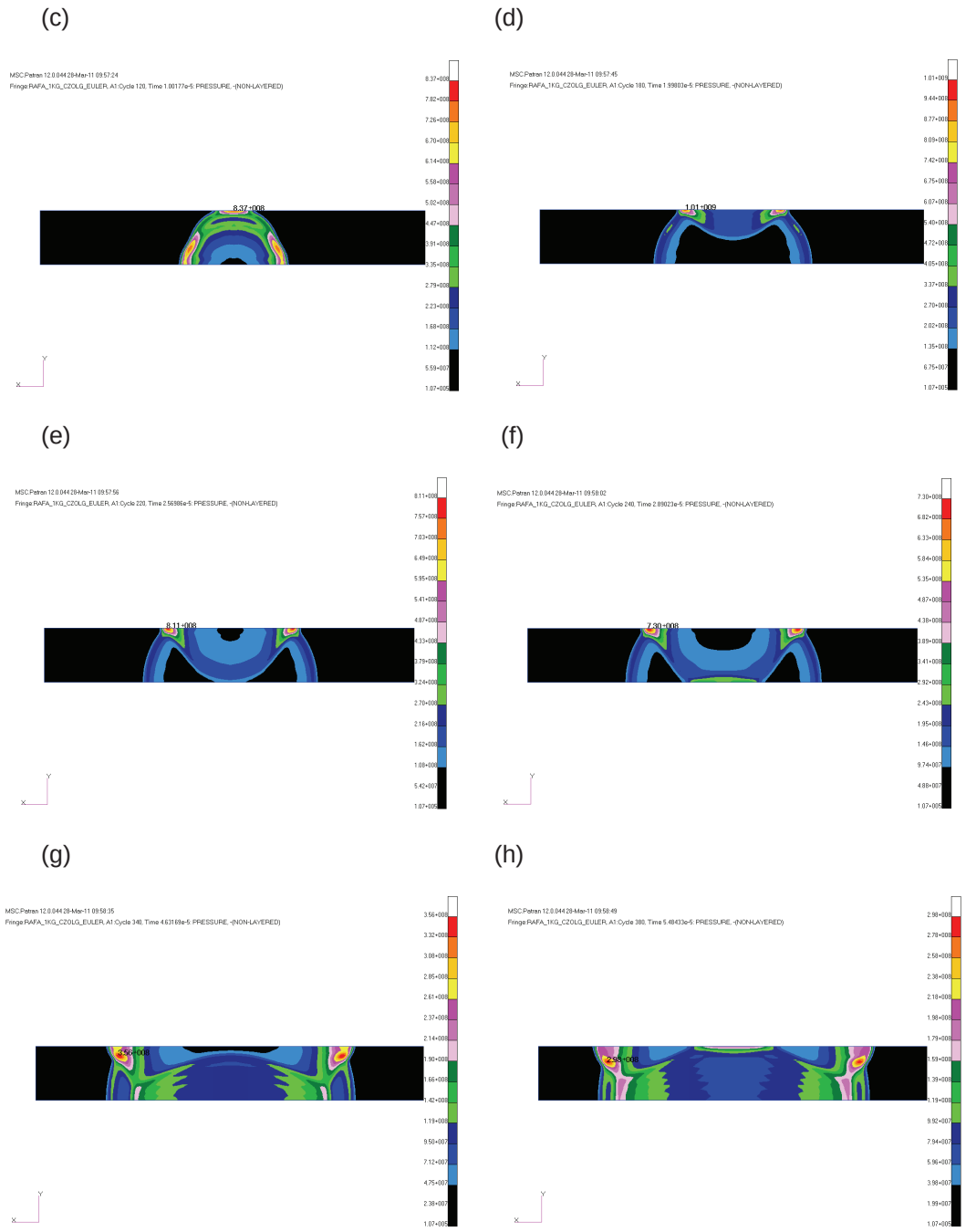


*Fig. 7. Wave propagation and reflections from the bottom and the ground in Model 2*

Figure 8 shows the pressure plots for Euler cells in Model 3 (with deflector). The maximum value of pressure in cell A was 4,5E9 Pa. This value was very similar to the one obtained in cell A in Model 2.

There was however, a small difference due to the difference in Euler cells shape. Elements in Model 3 were differently orientated as a result of deflector shape. Nevertheless, the element size was identical in both cases.

As a result of pressure wave propagation, the value in cell B decreased to 1,7 E9 Pa. In cell C the pressure was 8E8 and in D cell pressure reached 4,5 E8 Pa. Values for all B, C and D cells are two times lower than corresponding pressure values in Model 2. Therefore, the usage of the deflector decreases the overall pressure affecting the structure.

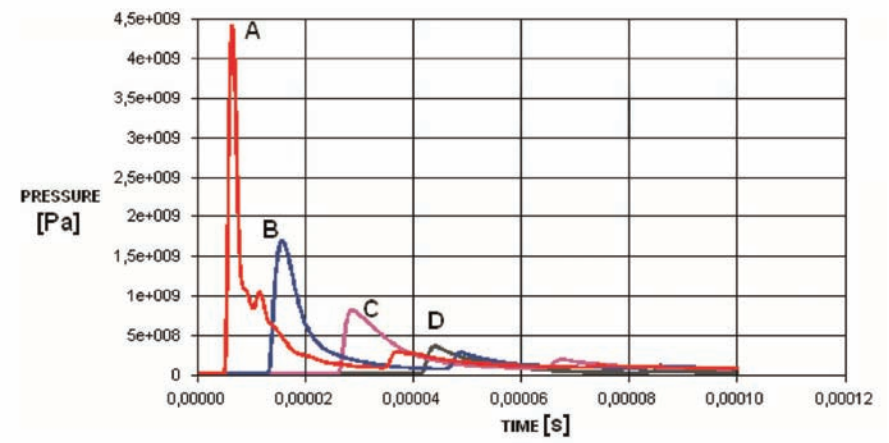


*Fig. 8. Model 3 – pressure values in cells A, B, C and D*

Considering pressure maps of Model 3 depicted in Fig. 9, one must notice multiple reflections similar to those in Model 2. For the time t = 9,43E7 s (a) pressure wave reached the ground.

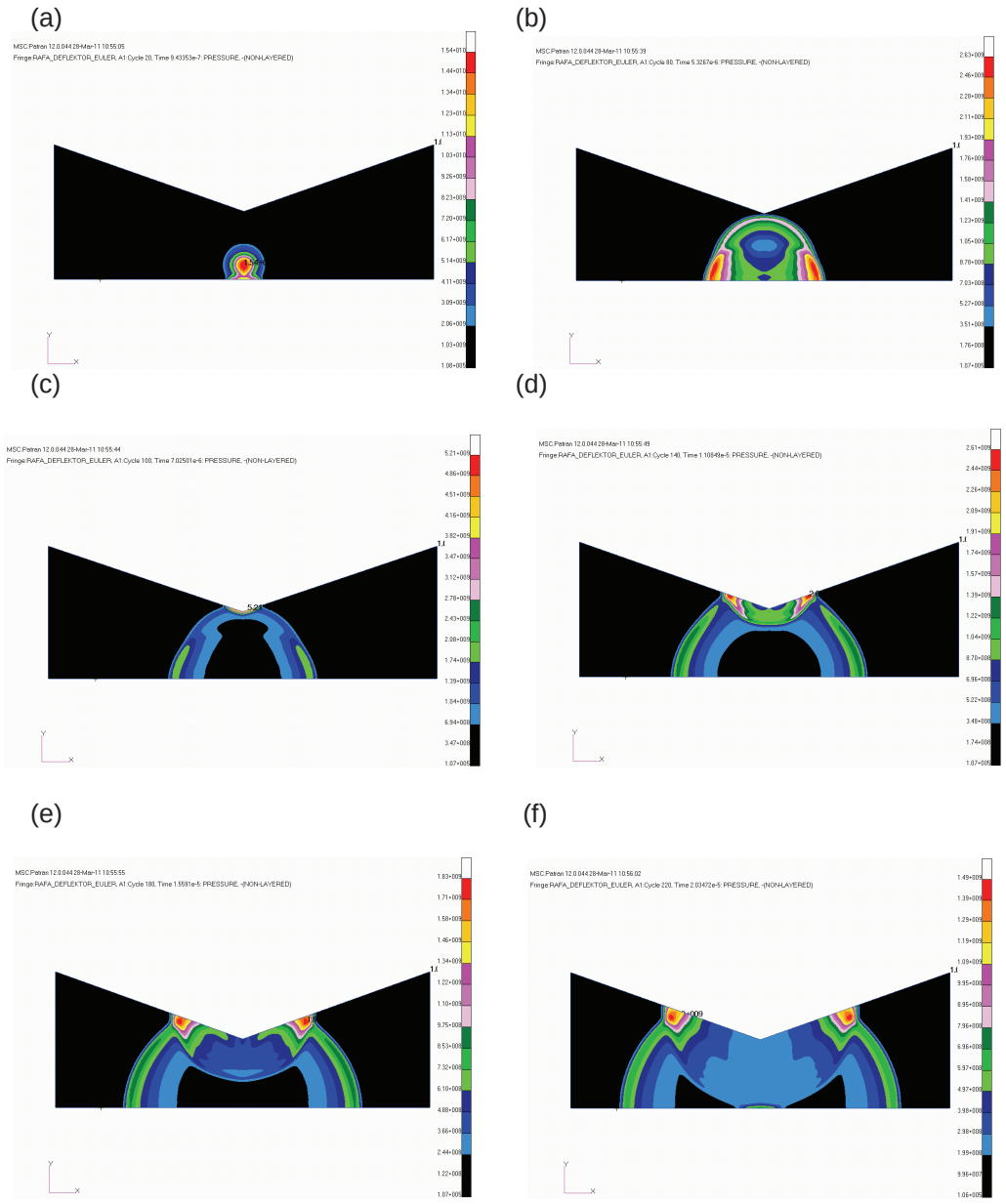

(g) (h)

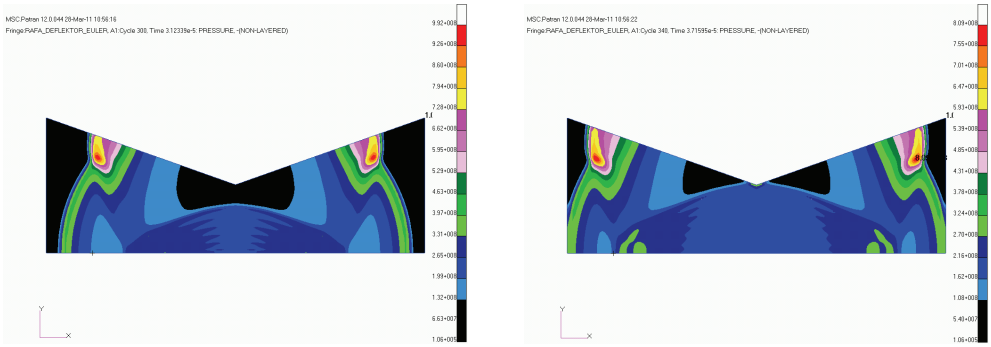

*Fig. 9. Blast wave propagation Ruth multiple reflections*

For the time t = 5.32 E-6 s the blast wave reached the deflector. As a result of the reflection, the pressure amplification was observed to the value 5,21E9 Pa. Afterwards, propagation is shown in Fig. 9d –f. Fig 9g and h show the creation of Mach's wave as a result of multiple reflections and intersection of incident and reflected waves.

## 4. Conclusions

In the article, the pressure wave propagation in Euler domain for three cases is presented - without any boundaries, with flat bottom and with a deflector. Introducing the boundaries resulted in an increase of the maximum value of the pressure impulse. Since the analyses were conducted for cubic but very dense Euler mesh, the maximum pressure on the wave front was only slightly affected by the mesh shape [11]. Usage of deflector decreases the maximum pressure affecting the vehicle's bottom two times. The work presented in the article is a part of broader research into the pressure wave's propagation. To obtain the pressure plot shape and values a model of the entire vehicle was used.

## References


[1] Barnat, W., *Transporter Opancerzony Adi Bushmaster*, Myśl Wojskowa 5/2005.

[2] Trzciński, W., Trębiński, R., Cudziło, S., *Investigation of the Behaviour of Steel and Laminated Fabric Plates Under Blast Wave Load*, Part I: Experimental Approach, V International Armament Conference, Waplewo 2005.

[3] Krzewiński, R., Rekrucki, R., *Roboty budowlane przy użyciu materiałów wybuchowych*, Polcen 2005.

[4] Thornton, P. H., Jeryan, R. A., *Crash Energy Management in Composite Automotive Structures*, International Journal of Impact Engineering, Vol. 7, No 2, pp. 167-180, 1988.

[5] Babul, W., *Odkształcanie metali wybuchem*, WNT Warszawa 1980.

[6] Włodarczyk, E., *Wstęp do mechaniki wybuchu*, PWN, Warszawa 1994.

[7] Dytran Theory Manual, 2004; LS-DYNA theoretical manual, 1998.

[8] Łęgowski, Z., Rafa, J., *Modelowanie wielokrotnych oddziaływań powybuchowych fal uderzeniowych na elementy konstrukcji*, I Konferencja odporność Udarowa Konstrukcji Gdynia 1993.

[9] Ls_Dyna Theory Manual, Livemore, CA, 2005.

[10] Baker, W. E., *Explosions in Air*, University of Texas Press, Austin and London 1973.

[11] Barnat, W., *Wybrane problemy energochłonności nowych typów paneli ochronnych obciążonych falą wybuchu*, BEL Studio, Warszawa 2010.

[12] Barnat, W., Panowicz, R., Niezgoda T., *Numerical investigation of the influence of a rigid obstacle on the multiple reflected pressure impulse*, Journal of KONES, Warsaw 2010.